Biophysical Chemistry 25 (1986) 27–36
Elsevier

BPC 01087

ELUTION-BAND RELAXATION METHOD

A METHOD TO ANALYZE ISOMERIZATION KINETICS BY HPLC AND APPLICATION TO PROTEIN DENATURATION-RENATURATION

Ryo HANAI, Shigeru ENDO * and Akiyoshi WADA

Department of Physics, Faculty of Science, University of Tokyo, Hongo, Bunkyo-ku, Tokyo 113, Japan

Received 13th April 1986
Revised manuscript received 9th July 1986
Accepted 11th July 1986

Key words: HPLC; Isomerization kinetics; Protein denaturation-renaturation; Ribonuclease A

We present a novel method, the 'elution-band relaxation method', to analyze quantitatively reversible isomerization kinetics by elution chromatography, taking advantage of the high resolution and speed of high-performance liquid chromatography (HPLC). The kinetic information is obtained by measuring the first temporal moments of chromatograms of molecules undergoing isomerization and analyzing their dependence on the column length or flow rate. The major advantage of this method is that it is applicable to reactions as fast as the time of elution in HPLC, a speed which has not been attained previously in analysis of isomerization reactions based on the chromatographic property of molecules. We describe the method and report an experimental application to the denaturation-renaturation kinetics of bovine pancreatic ribonuclease A as an example.

1. Introduction

High-performance liquid chromatography (HPLC) is well known as a powerful tool to separate biological macromolecules (for reviews, see refs. 1 and 2). It is, however, not fully recognized as a means of quantitative analysis in biophysical chemistry, although its potentiality was clearly demonstrated by 'zone-interference chromatography', a method for studying macromolecular interactions [3]. In the current study we present another example of the analytical potential of HPLC. We describe a novel method to study another biologically important reaction, isomerization, by HPLC, taking advantage of its high resolution and speed.

Many theoretical studies have been done on the spatial distribution of molecules under isomerization in mass transport systems [4–9]. Mitchell [8] has derived a rigorous solution of the partial differential equations which contain isomerization, mass transfer and diffusion. Experimental results from urea-gradient gel electrophoresis of proteins (for a review, see ref. 10) have been interpreted in terms of Mitchell's solution [11].

However, we cannot use the theory mentioned above because elution chromatography gives the temporal distribution but not the spatial distribution. We can transform spatial distribution into temporal distribution by a mathematical procedure, but in the present study we do not intend to develop a method of analysis using temporal distribution itself because such a method is expected to be complicated.

The strategy we follow in the present study is to focus on the first moment of the chromatogram. It has two major advantages. One is theoret-

* Present address: Biometrology Lab., JEOL Ltd., Nakagami, Akishimashi, Tokyo 196, Japan.

0301-4622/86/$03.50 © 1986 Elsevier Science Publishers B.V. (Biomedical Division)

ical: the high resolution of HPLC allows us to use a simple model. The other is experimental: it is easy to measure the first moments experimentally with high precision.

In the following we describe the principle and procedure of our method in detail, and report its experimental application to protein denaturation-renaturation as an example.

2. Theory

2.1. Model

We present a model to calculate the first temporal moment. In this model, molecule A moves with a velocity, v_A, and changes to B with a rate constant, k, at the same time. Molecule B moves with velocity v_B and changes to A with rate constant k'. This situation is expressed mathematically as [7]

$$\frac{\partial}{\partial t}\rho_A(x, t) = -v_A\frac{\partial}{\partial x}\rho_A(x, t) - k\rho_A(x, t) + k'\rho_B(x, t) \quad (1)$$

$$\frac{\partial}{\partial t}\rho_B(x, t) = -v_B\frac{\partial}{\partial x}\rho_B(x, t) + k\rho_A(x, t) - k'\rho_B(x, t), \quad (2)$$

where $\rho_A(x, t)$ is the spatial distribution of molecule A at time t and $\rho_B(x, t)$, that of molecule B. Diffusion terms can be neglected, as discussed later. The initial conditions are

$$\rho_A(x, t=0) = \delta(x) \quad (3)$$

$$\rho_B(x, t=0) = 0. \quad (4)$$

The point $x=0$ is taken to be the column entrance and the point $x=l$, the column end (i.e., l = column length).

We look upon the mass flow function, $v_A\rho_A + v_B\rho_B$, at $x=l$ as the elution chromatogram; we have the first temporal moment as

$$M_1(l) = \int_0^\infty t(v_A\rho_A + v_B\rho_B)\,dt. \quad (5)$$

2.2. Validity of the model

Here we show that diffusion terms can be neglected in considering the first moment of the HPLC chromatogram. We consider the following equation in an endless system [12–14]:

$$\frac{\partial}{\partial t}\rho(x, t) = D\frac{\partial^2}{\partial x^2}\rho(x, t) - v\frac{\partial}{\partial x}\rho(x, t). \quad (6)$$

D is the effective diffusion constant which includes mass transfer kinetics, ordinary molecular diffusion, eddy diffusion, etc. [14]. As the initial condition we take $\rho(x, t=0) = \delta(x)$. The first moment is (see appendix A)

$$M_1(l) = \int_0^\infty t\left(v\rho(l, t) - D\frac{\partial}{\partial x}\rho(l, t)\right)dt = \frac{l}{v}\left(1 + \frac{D}{vl}\right), \quad (7)$$

where l/v is the time to travel a length l with a velocity v; the correction for diffusion is D/lv. According to plate theory, $2D/v$ is the height equivalent to a theoretical plate [12–14]; D/vl equals the reciprocal of twice the number of theoretical plates. In HPLC the number is usually of the order of 10^3, 10^4 or larger; D/vl is negligibly small.

We would like to make two more comments on the diffusion effect. (1) Although we can take another boundary condition for eq. 6 which seems more realistic [15], the conclusion that the diffusion effect is negligible is not altered. (2) We can calculate the first temporal moment in the case of an irreversible reaction in an endless system, taking diffusion terms into account (see appendix B).

2.3. Calculation of the first moment

We calculate the first moment, using Laplace transformation. Eq. 5 can be expressed as

$$M_1(l) = -\frac{d}{d\kappa}(v_A\mathscr{L}_A + v_B\mathscr{L}_B)\Big|_{\kappa=0}, \quad (8)$$

where $\mathscr{L}_A$ and $\mathscr{L}_B$ are the Laplace transformations of ρ_A and ρ_B, respectively:

$$\mathscr{L}_A(\kappa) = \int_0^\infty e^{-\kappa t}\rho_A\,dt \quad (9)$$

$$\mathscr{L}_B(\kappa) = \int_0^\infty e^{-\kappa t}\rho_B\,dt. \quad (10)$$

Instead of eqs. 1 and 2 we have

$$\kappa\mathscr{L}_A = -v_A\frac{d}{dx}\mathscr{L}_A - k\mathscr{L}_A + k'\mathscr{L}_B \tag{11}$$

$$\kappa\mathscr{L}_B = -v_B\frac{d}{dx}\mathscr{L}_B + k\mathscr{L}_B - k'\mathscr{L}_A, \tag{12}$$

and for eqs. 3 and 4

$$\mathscr{L}_A(x=0) = \int_0^\infty e^{-\kappa t}(v_A\kappa_A + v_B\rho_B)\,dt\Big|_{\kappa=0} = 1/v_A \tag{13}$$

$$\mathscr{L}_B(x=0) = 0 \tag{14}$$

as the initial conditions for eqs. 11 and 12. Putting the solutions of $\mathscr{L}_A$ and $\mathscr{L}_B$ into eq. 8, we obtain

$$M_1(l) = \frac{k}{v_A}\frac{\frac{1}{v_A}-\frac{1}{v_B}}{\left(\frac{k}{v_A}+\frac{k'}{v_B}\right)^2}\times\left[1-\exp\left(-\left(\frac{k}{v_A}+\frac{k'}{v_B}\right)l\right)\right] + \frac{k+k'}{v_Bk+v_Ak'}l. \tag{15}$$

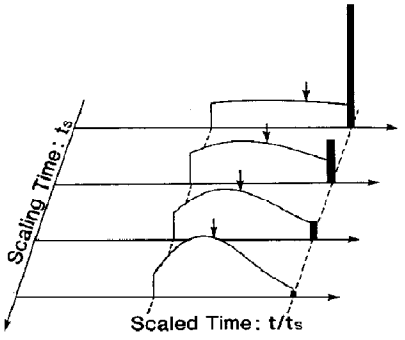

Fig. 1. Principle of the elution-band relaxation method. The scaling time is the characteristic time of operation. As the scaling time increases, the remaining peak of the injected material, indicated by black bars, becomes smaller, and a broad band grows, resulting from isomerized molecules. The method analyzes this elution-band relaxation by evaluating the shift of the first moment, indicated by arrows and obtains the rate constants.

2.4. Method of application

2.4.1. Elution-band relaxation method

We discuss a method for obtaining the kinetic constants, k and k', from the experimentally obtained first moment, which we call the elution-band relaxation method.

To show the physical picture of the method, we rewrite eq. 15 as follows. Let v, a velocity or a velocity analogue that is characteristic of the system (e.g., the flow rate), and t_S be defined by $t_S = l/v$, the characteristic time of operation, the scaling time; and we have

$$M_1(t_S) = \frac{k}{r_A}\frac{\frac{1}{r_A}-\frac{1}{r_B}}{\left(\frac{k}{r_A}+\frac{k'}{r_B}\right)^2}\times\left[1-\exp\left(-\left(\frac{k}{r_A}+\frac{k'}{r_B}\right)t_S\right)\right] + \frac{k+k'}{r_Bk+r_Ak'}t_S, \tag{16}$$

where $r_A = v_A/v$ and $r_B = v_B/v$.

The physical implication of this equation is depicted by introducing two time axes (fig. 1): one is the axis of the scaling time and the other is that of the scaled time which is the real time divided by the scaling time. At a fixed scaling time one chromatogram is obtained on the scaled time axis. Fig. 1 is a simulation of elution chromatograms of molecules under isomerization. The black bars indicate the remained peaks of injected molecules. The longer the scaling time, the smaller the peak becomes because more molecules have isomerized. In addition, the isomerized molecules form a broad band resulting from further isomerization. In this sense the elution band relaxes and the scaled moment ($M_1(t_S)/t_S$, indicated by arrows in fig. 1) shifts. Our method is to analyze this elution-band relaxation by evaluating the shift of the first moment and to obtain the kinetic constants of the reaction.

Next we describe the procedure followed in the method. We rewrite eq. 16 simply as

$$M_{1A}(t_S) = \alpha_A(1-e^{-\beta t_S}) + \gamma t_S, \tag{17}$$

where

$$\alpha_A = \frac{k}{r_A} \cdot \frac{\frac{1}{r_A} - \frac{1}{r_B}}{\left(\frac{k}{r_A} + \frac{k'}{r_B}\right)^2} \tag{18}$$

$$\beta = \frac{k}{r_A} + \frac{k'}{r_B} \tag{19}$$

$$\gamma = \frac{k + k'}{r_B k + r_A k'}. \tag{20}$$

The suffix A means that A molecules were injected. To determine all the four parameters (v_A, v_B, k and k') we must also measure $M_{1B}(t_S)$: the first moment obtained by injecting B. We obtain $M_{1B}(t_S)$ by exchanging k and k', and r_A and r_B in eq. 16:

$$M_{1B}(t_S) = \alpha_B(1 - e^{-\beta t_S}) + \gamma t_S, \tag{21}$$

where

$$\alpha_B = \frac{k'}{r_B} \cdot \frac{\frac{1}{r_B} - \frac{1}{r_A}}{\left(\frac{k}{r_A} + \frac{k'}{r_B}\right)^2}. \tag{22}$$

The unknown parameters (α_A, α_B, β and γ) can be determined by measuring $M_{1A}(t_S)$ and $M_{1B}(t_S)$ for various values of t_S and by least-squares analysis. A series of t_S may be obtained by varying l and/or v. The rate constants and the velocities are calculated as

$$k = \frac{\alpha_A \beta}{(\alpha_A \beta + \gamma)(\alpha_A - \alpha_B)} \tag{23}$$

$$k' = \frac{\alpha_B \beta}{(\alpha_B \beta + \gamma)(\alpha_B - \alpha_A)} \tag{24}$$

$$v_A = v/(\alpha_A \beta + \gamma) \tag{25}$$

$$v_B = v/(\alpha_B \beta + \gamma). \tag{26}$$

2.4.2. Simplified procedure

Here we describe another procedure, the 'simplified procedure', where v_A and v_B are assumed to be known. They can be approximated from the positions of the remaining peaks of the injected material. When M_{1A} and M_{1B} have been measured for one value of t_S, the following equation of x must be solved:

$$\frac{1 - e^{-x}}{x} = \frac{M_{1A} - M_{1B}}{t_A - t_B}, \tag{27}$$

where t_A and t_B are the elution times of the peaks of A and B, respectively. k and k' are calculated as

$$k = \frac{x(M_{1A} - t_A)}{t_A(M_{1A} - M_{1B} + t_A - t_B)} \tag{28}$$

$$k' = \frac{x(M_{1B} - t_B)}{t_B(M_{1B} - M_{1A} + t_B - t_A)}. \tag{29}$$

2.5. Feasibility

Here we discuss the feasibility of our method briefly. The method is feasible when the unknowns (α_A, α_B, β and γ) can be determined. For this the following conditions are found to be satisfied: (1) α_A and α_B are large. (2) $\beta t_S \approx 1$.

Condition 1 is equivalent to the following conditions (see eq. 18–20 and 22): (i) k and k' are small enough. (ii) $k \sim k'$. (iii) Velocities of isomers are different. How much difference is necessary depends on the HPLC system. As to k, however, condition 2 gives another condition:

$$\frac{1}{k} \approx \frac{l}{v_A}\left(1 + \frac{v_A k'}{v_B k}\right),$$

i.e., the time constant of the reaction should be comparable to the time of elution. k' should satisfy a similar condition.

3. Experimental

We applied our method to the denaturation-renaturation kinetics of bovine pancreatic ribonuclease A (RNase A) in guanidium chloride (GuHCl) solution. We used a gel permeation column to analyze the reaction by the 'size' of the protein molecule.

In this section we denote the native protein as A and the denatured protein as B, the rate constant of denaturation as k and that of renaturation as k'.

3.1. Materials and methods

3.1.1. Materials

RNase A (XII-A) was purchased from Sigma Chemicals (St. Louis). For HPLC experiments further purification was done on TSK-G2000SW (7.5 mm × 60 cm, Toyo Soda, Tokyo) to remove contaminants completely. Lyophilized powder of protein containing buffer salts was dissolved in water to yield native protein solution or in 5 M GuHCl, 50 mM Tris-HCl, pH 7.6, to yield denatured protein solution. The denatured protein eluted as a single band in 5 M GuHCl. GuHCl (specially prepared grade) was from Nakarai Chemicals (Kyoto). Tris (T-1503) was from Sigma. The concentration of GuHCl was determined by means of an Abbe refractometer [16].

3.1.2. HPLC

The pump system was an HLC-803D (Toyo Soda) and the column a TSK-G2000SW (7.5 mm × 60 cm, Toyo Soda). The injection volume was 10 μl. Chromatograms were monitored using an absorbance detector (UV-8, Toyo Soda) at 230 nm where the absorbance of RNase A varies little before and after denaturation. Data were A/D converted every second and stored on a floppy disk by a microcomputer. Flow rates were determined from the positions of the ghosts by taking a flow rate of 1 ml/min as standard.

3.1.3. Optical

Optical measurements were made on our multidimensional spectrophotometer (Mark-III) [17]. A GuHCl jump was performed by mixing 0 M GuHCl and 5 M GuHCl solution. Mixing was done by injecting buffer into the protein solution in the optical cell and stirring with a magnetic stirrer.

3.2. Results and discussion

3.2.1. Denaturation-renaturation kinetics of RNase A

We first show the results of the study on the denaturation-renaturation kinetics of RNase A, in 3 M GuHCl, 50 mM Tris-HCl, pH 7.6, at 20°C. The scaling time, t_S, was changed by varying the flow rate.

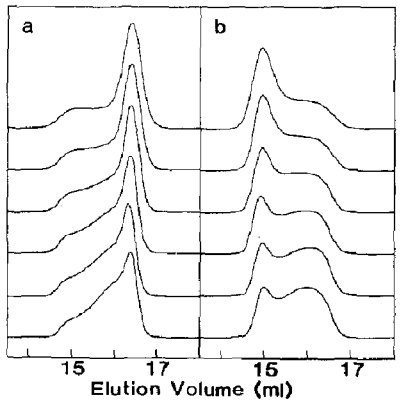

Fig. 2. Chromatograms of RNase A under denaturation-renaturation in 3 M GuHCl, 50 mM Tris, pH 7.6, 20°C. The column was TSK-G2000SW (7.5 mm × 60 cm, Toyo Soda). Starting material was (a) native protein and (b) denatured protein. The flow rates were (a) 1.00, 0.706, 0.511, 0.412, 0.344 and 0.296 ml/min and (b) 1.00, 0.708, 0.511, 0.412, 0.345 and 0.296 ml/min from above, respectively. Chromatograms are normalized to give the same area.

Chromatograms are shown in fig. 2 for the elution volume. The number of theoretical plates was estimated at 6500 from the width of the right-hand side of the peak of the uppermost chromatogram in fig. 2a [12].

The first moment in the elution volume is plotted vs. 1/flow rate in fig. 3. As can be easily

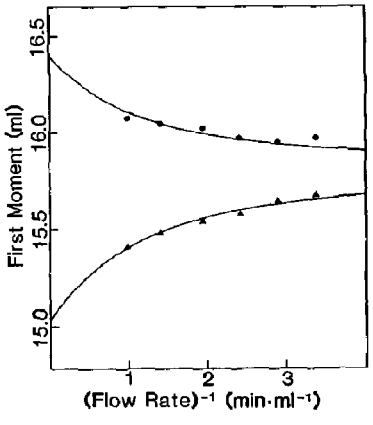

Fig. 3. First moment in elution volume vs. 1/flow rate, calculated from the chromatograms of fig. 2: (●) fig. 2a, (▲) fig. 2b.

seen, this plot is equivalent to the plot of $M_1(t_S)/t_S$ vs. t_S. The results of the least-squares analysis are $v_A = 3.66 \pm 0.01$ cm min^{-1}, $v_B = 3.99 \pm 0.02$ cm min^{-1}, $k = 0.039 \pm 0.03$ min^{-1}, $k' = 0.057 \pm 0.05$ min^{-1}. Values of the velocities are given for a flow rate of 1 ml/min and agree with those calculated from the peak positions of the chromatograms of this flow rate in fig. 2 ($v_A = 3.65$ cm/min and $v_B = 4.01$ cm/min), supporting the consistency of the analysis.

3.2.2. Denaturant concentration dependence of denaturation-renaturation of RNase A

Next we provide the results from the study on the GuHCl concentration dependence of the kinetics by the simplified procedure.

The results are summarized in table 1. The activation free energy was calculated from $\Delta G^{\ddagger} = -RT \ln(kh/k_B T)$ and is shown in fig. 4. The free energy of denaturation was also calculated from $\Delta G = -RT \ln(k/k')$ and is shown in fig. 5. By extrapolation of the line in fig. 5 the ΔG value at 0 M GuHCl was estimated at 6.9 kcal/mol.

It was a good approximation to obtain v_A and v_B from the peak positions of the chromatogram because (1), as seen in fig. 2, the peak position was almost independent of the progress of reaction and (2) the velocities calculated from the peak positions agreed with those from the least-square fitting.

Table 1

GuHCl concentration dependence of denaturation-renaturation kinetics of RNase A

Other solvent condition than GuHCl was 50 mM Tris-HCl, pH 7.6, 20°C. The simplified procedure was used. The flow rate was 1.0 ml/min.

[GuHCl] (M)	Denaturation rate constant, k (min^{-1})	Renaturation rate constant, k' (min^{-1})	Equilibrium constant of denaturation, k/k'
2.8	0.034	0.10	0.35
3.0	0.047	0.068	0.70
3.2	0.084	0.048	1.7
3.4	0.13	0.039	3.3

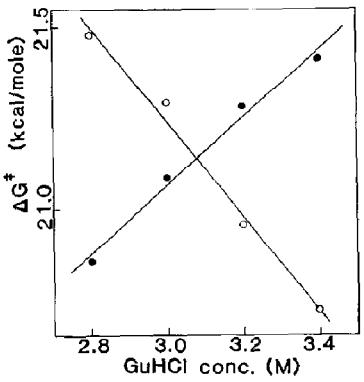

Fig. 4. Activation free energy of denaturation (○) and renaturation (●) of RNase A by GuHCl in 50 mM Tris, pH 7.6, at 20°C.

3.2.3. Comparison with the results of optical measurement

To compare our results by HPLC with those by another method, we studied the kinetics by circular dichroism (CD) and fluorescence. So far the renaturation kinetics of RNase A has been studied mainly by absorbance measurement, and the results have been interpreted by a sequential scheme which comprises an intermediate [18] or by a model which assumes many unfolded states [19].

The kinetics was studied by means of GuHCl jumps from 0 to 3 M, and from 5 to 3 M. Fig. 6 shows an example of the data. No significant change in CD intensity was observed within the dead time of mixing in any experiment. The corre-

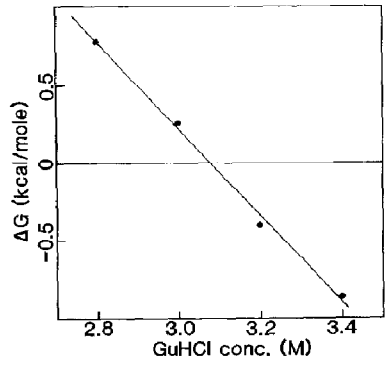

Fig. 5. Free energy of denaturation of RNase A by GuHCl in 50 mM Tris, pH 7.6, at 20°C.

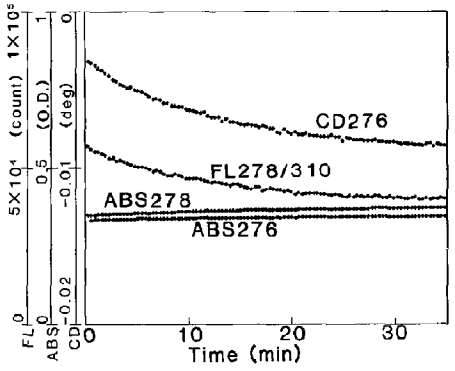

Fig. 6. Example of data of denaturation-renaturation kinetics of RNase A in 50 mM Tris, 3 M GuHCl, pH 7.6, at 20°C. In this example the GuHCl concentration was changed from 5 to 3 M. Signals were observed simultaneously. Numbers after CD or ABS (Absorbance) indicate the wavelengths; FL278/310 is the fluorescence excited at 278 nm and detected at 310 nm.

lation plots, drawn in fig. 7, are linear and suggest that the secondary and tertiary structures of RNase A grow or are disrupted at the same time in 3 M GuHCl, 50 mM Tris-HCl, pH 7.6, at 20°C.

Fluorescence data were fitted by least squares to a single exponential $(a \times \exp(-\lambda t) + b)$. The results obtained were $\lambda = 0.0836 \pm 0.0015$ min^{-1} (from 0 to 3 M) and $\lambda = 0.0956 \pm 0.0020$ min^{-1} (from 5 to 3 M). The residuals showed no systematic distribution. The discrepancy of the λ values may result from the precision of the control of the temperature (± 1°C).

The denaturation-renaturation of RNase A in 3 M GuHCl, 50 mM Tris-HCl, pH 7.6, at 20°C is well characterized by a two-state reaction because (1) the changes in the far- and near-UV CD correlate linearly and (2) the kinetic data were well fitted by a single exponential and the rate constants were similar in both directions of the GuHCl jump. One can also find in the literature [20] an example showing that the renaturation of RNase A is a two-state process when detected by absorbance.

λ is equal to $k + k'$, which was 0.096 ± 0.006 min^{-1} in the HPLC study. The free energy of denaturation at 0 M GuHCl was 6.9 kcal/mol in the present HPLC study, which roughly agrees with the value of 10.3 kcal/mol in 50 mM Tris-HCl, pH 7.6, at 25°C determined by CD measurement [21]. From these agreements it is concluded that HPLC and optical measurement detected the

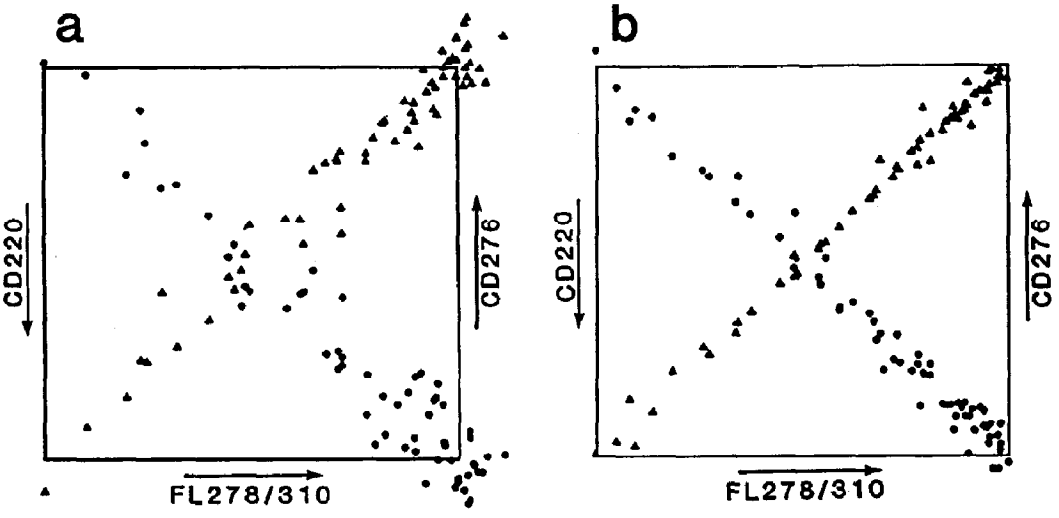

Fig. 7. Correlation plots of the kinetic data. The correlation between CD220 and FL278/310 (circles, from upper left to lower right) and FL278/310 and CD276 (triangles, from lower left to upper right). The GuHCl concentration was changed (a) from 0 to 3 M or (b) from 5 to 3 M. The time range of the plot was 35 min for both. Arrows indicate the directions of the changes of signals, i.e., time. CD276 and FL278/310 were measured simultaneously and CD220 was measured in another experiment. Plots were made by adjusting the time interval of measurement of CD276 and FL278/310 to that of CD220 by interpolation.

same process in the denaturation-renaturation of RNase A, although denaturation may be restricted when the protein molecule is in the pore of the gel [22].

4. Discussion

In the present study we have described a quantitative method to analyze isomerization kinetics on HPLC. It takes advantage of the high performance of HPLC in two points. Namely, (1) the high resolution of HPLC allows us to use a simple method of analysis which is applicable to reactions whose time constants are comparable to the time of elution. Other methods (e.g., optical methods) have a higher time resolution, but our method utilizes the chromatographic property of the molecule, which has not been used in the analysis of isomerization kinetics. (2) The speed of HPLC enables us to analyze fast reactions, which would be impossible by conventional liquid chromatography. Through these advantages we could study the denaturation-renaturation kinetics of protein using the 'size' of the molecule as a probe for the first time.

Our method is expected to have a wide range of application. Separation of isomers of dipeptides containing proline [23] and anomers of peptidoglycans [24] by reversed-phase liquid chromatography has been reported. It would then be possible to analyze kinetics as fast as a few minutes [23]. Our method would also be applicable to isomerization reactions consisting of more than two isomers, which may require more sophisticated procedures and/or higher resolution.

The success of our method in application is due not only to the high performance of HPLC but also to the highly quantitative nature of the chromatographic system equipped with a microprocessor in data acquisition and processing; it is difficult to attain such quantitative sophistication with an electrophoretic method [25]. Recently, such an HPLC system has become commercially available, and its analytical potential would be easily educed by software to reduce data.

So far sophisticated mathematics has been applied mainly to the mechanism of separation (e.g., refs. 14, 26 and 27). It has, however, turned out to be very fruitful in developing new analytical usages of HPLC in the work of Endo and Wada [3] and in the present study. We expect further developments in this field through the 'methods of mathematical physics' [28,29].

In conclusion, we would like to stress that the analytical potential of HPLC should be more widely exploited. Now HPLC is not a mere tool of separation but a 'spectrometer'.

Appendix A

The solution of eq. 6 is

$$\rho(x, t) = \frac{1}{\sqrt{4\pi Dt}} \exp\left[-\frac{(x-vt)^2}{4Dt}\right]. \tag{A1}$$

We obtain the mass flow at $x = l$ as

$$v\rho - D\frac{\partial}{\partial x}\rho\Big|_{x=l} = \frac{1}{\sqrt{4\pi D}}\left(\frac{v}{2\sqrt{t}} + \frac{l}{2t\sqrt{t}}\right) \times \exp\left[-\frac{(l-vt)^2}{4Dt}\right]. \tag{A2}$$

In calculating eq. 7, we use the formula [30]:

$$\int_0^\infty x^{\nu-1} \exp\left[-\left(\frac{\mu}{2}\right)^2 \frac{1}{x}\right] dx = 2\left(\frac{\mu}{2}\right)^\nu K_{-\nu}(\mu) \quad \left(|\arg \mu| < \pi/2,\ \mathrm{Re}(\mu^2) > 0\right), \tag{A3}$$

where $K_\nu(\mu)$ is the modified Bessel function of the second kind and for $\nu = n + 1/2$

$$K_{-(n+1/2)}(z) = \sqrt{(\pi/2z)}\, e^{-z} \sum_{r=0}^{n} \frac{(n+r)!}{r!(n-r)!(2z)^r} \tag{A4}$$

This method of calculation is applicable to the moment of arbitrary order.

Appendix B

We consider a system described by

$$\frac{\partial}{\partial t}\rho_A(x, t) = D_A\frac{\partial^2}{\partial x^2}\rho_A(x, t) - v_A\frac{\partial}{\partial x}\rho_A(x, t) - k\rho_A(x, t) \tag{B1}$$

$$\frac{\partial}{\partial t}\rho_B(x,t) = D_B\frac{\partial^2}{\partial x^2}\rho_B(x,t) - v_B\frac{\partial}{\partial x}\rho_B(x,t) + k\rho_A(x,t). \quad \text{(B2)}$$

The solution was given by Mitchell [8] as

$$\rho_A(x,t) = \frac{1}{\sqrt{4\pi Dt}}\exp\left[-\frac{(x-vt)^2}{4Dt} - kt\right] \quad \text{(B3)}$$

$$\rho_B(x,t) = \int_0^t \frac{k\,dt_1}{\sqrt{4\pi D_A t_1 + 4\pi D_B(t-t_1)}} \times \exp\left[-\frac{\{x-(v_A t_1 + v_B(t-t_1))\}^2}{4D_A t_1 + 4D_B(t-t_1)} - kt_1\right]. \quad \text{(B4)}$$

The first moment is

$$M_1(l) = \int_0^\infty t\left(v_A\rho_A(l,t) - D_A\frac{\partial}{\partial x}\rho(l,t) + v_B\rho_B(l,t) - D_B\frac{\partial}{\partial x}\rho(l,t)\right)dt. \quad \text{(B5)}$$

We rewrite eq. B4 as

$$\rho_B(x,t) = \int_{-\infty}^{\infty} dx' \int_0^t dt_1 \frac{1}{\sqrt{4\pi D_A t_1}}\exp\left[-\frac{(x'-vt_1)^2}{4D_A t_1}\right] \times \frac{1}{\sqrt{4\pi D_B(t-t_1)}} \times \exp\left[-\frac{\{(x-x') - v_B(t-t_1)\}^2}{4D_B(t-t_1)} - kt_1\right]. \quad \text{(B6)}$$

put eqs. B3 and B6 into eq. B5, exchange the order of integration so that $\int_{-\infty}^{\infty} dx'$ may be the last one, and transform the integrand $\int_0^\infty dt \int_0^t dt_1$ into $\int_0^\infty dt \int_0^\infty dT$ by $T = t - t_1$. Using the formulae, eqs. A3 and A4, we have

$$M_1(l) = \left[\frac{D_B}{v_e v_B^2}\left\{\frac{k}{\frac{v_e - v_A}{2D_A} + \frac{v_B}{D_B}} - \tfrac{1}{2}(v_A + v_e)\right\} + \frac{D_A}{v_e(v_e - v_A)}\left(\frac{v_A + v_e}{v_B} - 2\right)\right] \times \exp\left(\frac{-l}{2D_A}(v_e - v_A)\right) + \frac{l}{v_B} + \frac{4D_A}{v_e^2} + \frac{D_B}{v_B^2} + \frac{v_A}{v_e k}\left(\frac{v_A}{v_e} - \frac{v_c}{v_B}\right), \quad \text{(A11)}$$

where

$$v_e = \sqrt{v_A^2 + 4D_A k}\,.$$

Acknowledgment

This work was partially supported by a Grant-in-Aid for Special Project Research No. 6113001 from the Ministry of Education, Science, and Culture of Japan.

References

1 F.E. Regnier, Science 222 (1983) 245.
2 F.E. Regnier, Methods Enzymol. 91 (1983) 137.
3 S. Endo and A. Wada, Biophys. Chem. 18 (1983) 291.
4 J.R. Cann, J.G. Kirkwood and R.A. Brown, Arch. Biochem. Biophys. 72 (1957) 37.
5 P.C. Scholten, Arch. Biochem. Biophys. 93 (1961) 568.
6 J.R. Cann and H.R. Bailey, Arch. Biochem. Biophys. 93 (1961) 576.
7 K.E. Van Holde, J. Chem. Phys. 37 (1962) 1922.
8 R.M. Mitchell, Biopolymers, 15 (1976) 1717, 1741.
9 M.K. Killalea and B.J. McCoy, Biopolymers, 19 (1980) 1875.
10 D.P. Goldenberg and T.E. Creighton, Anal. Biochem. 138 (1984) 1.
11 T.E. Creighton, J. Mol. Biol. 129 (1979) 235.
12 A.J.P. Martin and R.L.M. Synge, Biochem. J. 35 (1941) 1358.
13 E. Glueckauf, Trans. Faraday Soc. 51 (1955) 34.
14 J.C. Giddings, Dynamics of chromatography, part I, Principles and theory (Marcel Dekker, New York, 1965).
15 H.W. Hethcote and C. DeLisi, J. Chromatogr. 240 (1982) 269.
16 Y. Nozaki, Methods Enzymol. 26 (1972) 43.
17 A. Wada, H. Tachibana, H. Hayashi and Y. Saito, J. Biochem. Biophys. Methods 2 (1980) 257.

18 F.X. Schmid, Biochemistry 22 (1983) 4690.
19 L.-N. Lin and J.F. Brandts, Biochemistry 23 (1984) 5713.
20 H. Krebs, F.X. Schmid and R. Jaenicke, Biochemistry 24 (1985) 3846.
21 Y. Saito, D. Sci. Thesis, University of Tokyo, Japan (1982).
22 E.B. Zhulina and T.M. Brishtein, Mol. Biol. (U.S.S.R.) 16 (1982) 1322 (English Translation (1983) 1066).
23 W.R. Melander, J. Jacobson and C. Horváth, J. Chromatogr. 234 (1982) 269.
24 M. Lebl and V. Gut, J. Chromatogr. 260 (1983) 478.
25 S. Endo, Y. Saito and A. Wada, Anal. Biochem. 131 (1983) 108.
26 F.C. Denizot and M.A. Delaage, Proc. Natl. Acad. Sci. U.S.A. 72 (1975) 4840.
27 C. Horváth and H.-J. Lin, J. Chromatogr. 149 (1978) 43.
28 R. Courant and D. Hilbert, Methods of mathematical physics, vol. 1 (Interscience, New York, 1953).
29 R. Courant and D. Hilbert, Methods of mathematical physics, vol. 2 (Interscience, New York, 1962).
30 I.S. Gradshteyn and I.M. Ryzhik, Tables of integrals, series, and products (Academic Press, London, 1980).